

Role of the Macrophage Inflammatory Protein-1 α /CC Chemokine Receptor 5 Signaling Pathway in the Neuroinflammatory Response and Cognitive Deficits Induced by β -Amyloid Peptide

Giselle Fazzioni Passos, Cláudia Pinto Figueiredo, Rui Daniel Schröder Prediger, Pablo Pandolfo, Filipe Silveira Duarte, Rodrigo Medeiros, and João B. Calixto

From the Departamento de Farmacologia, Centro de Ciências Biológicas, Universidade Federal de Santa Catarina, Florianópolis, Santa Catarina, Brazil

The hallmarks of Alzheimer's disease include the deposition of β -amyloid ($A\beta$), neuroinflammation, and cognitive deficits. The accumulation of activated glial cells in cognitive-related areas is critical for these alterations, although little is known about the mechanisms driving this event. Herein we used macrophage inflammatory protein-1 α (MIP-1 $\alpha^{-/-}$)- or CC-chemokine receptor 5 (CCR5 $^{-/-}$)-deficient mice to address the role played by chemokines in molecular and behavioral alterations induced by $A\beta_{1-40}$. $A\beta_{1-40}$ induced a time-dependent increase of MIP-1 α mRNA followed by accumulation of activated glial cells in the hippocampus of wild-type mice. MIP-1 $\alpha^{-/-}$ and CCR5 $^{-/-}$ mice displayed reduced astrogliosis and microgliosis in the hippocampus after $A\beta_{1-40}$ administration that was associated with decreased expression of cyclooxygenase-2 and inducible nitric oxide synthase, as well as reduced activation of nuclear factor- κ B, activator protein-1 and cyclic AMP response element-binding protein. Furthermore, MIP-1 $\alpha^{-/-}$ and CCR5 $^{-/-}$ macrophages showed impaired chemotaxis *in vitro*, although cytokine production in response to $A\beta_{1-40}$ was unaffected. Notably, the cognitive deficits and synaptic dysfunction induced by $A\beta_{1-40}$ were also attenuated in MIP-1 $\alpha^{-/-}$ and CCR5 $^{-/-}$ mice. Collectively, these results indicate that the MIP-1 α /CCR5 signaling pathway is critical for the accumulation of activated glial cells in the hippocampus and, therefore, for the inflammation and cognitive failure induced by $A\beta_{1-40}$. Our data suggest MIP-1 α and CCR5 as potential therapeutic targets for Alzheimer's dis-

ease treatment. (Am J Pathol 2009, 175:1586–1597; DOI: 10.2353/ajpath.2009.081113)

Alzheimer's disease (AD) is the most prevalent cause of dementia in humans, and the symptoms are commonly manifested after the seventh decade of life. Numerous pathological changes have been described in the post-mortem brains of AD patients, including senile plaques, tangles, neuroinflammation, synapse loss, and neuronal death.¹ Activated glial cells surrounding senile plaques seem to be responsible for the ongoing neuroinflammatory process in the disease through the release of cytokines and other toxic products, including reactive oxygen species, nitric oxide, and excitatory amino acids.² However, little is known about the identity of the agent(s) responsible for glial cell accumulation and activation in the AD brain.

Chemokines belong to a family of chemoattractant cytokines that were initially identified according to their ability to regulate leukocyte trafficking during inflammatory responses.^{3,4} More recently, in addition to their chemotactic activity, chemokines have been implicated in the modulation of cell adhesion, phagocytosis, cytokine secretion, proliferation, apoptosis, angiogenesis, and vi-

Supported by grants from the Conselho Nacional de Desenvolvimento Científico e Tecnológico (CNPq), the Coordenação de Aperfeiçoamento de Pessoal de Nível Superior, the Programa de Apoio aos Núcleos de Excelência, and the Fundação de Apoio a Pesquisa do Estado de Santa Catarina, all from Brazil. G.F.P. and P.P. are Ph.D. students in pharmacology receiving grants from CNPq. F.S.D. and R.M. hold postdoctoral fellowships from CNPq.

Accepted for publication July 9, 2009.

Supplemental material for this article can be found on <http://ajp.amjpathol.org>.

Address reprint requests to Prof. J. B. Calixto, Departamento de Farmacologia, Universidade Federal de Santa Catarina, Campus Universitário, Trindade, Bloco D, CCB, Caixa Postal 476, CEP 88049-900, Florianópolis, Santa Catarina, Brazil. E-mail: calixto@farmaco.ufsc.br or calixto3@terra.com.br.

ral pathogenesis.⁵ In the central nervous system (CNS), these proteins regulate leukocyte migration across the brain endothelium as well as the activation and movement of cells within the brain parenchyma.⁶ There is growing evidence supporting the view that resident CNS cells have the capacity to express chemokines and their receptors during a variety of neuroinflammatory and degenerative conditions.^{7–14} Notably, recent evidence has indicated that chemokines and their receptors are up-regulated in the AD brain and that they may play a critical role in controlling the recruitment and accumulation of glial cells at β -amyloid ($A\beta$) sites in senile plaques.¹⁵

Macrophage inflammatory protein (MIP)-1 α (CCL3) is a member of the β -chemokine subfamily, which also includes MIP-1 β (CCL4) and regulated on activation, normal T-cell expressed and secreted (RANTES, CCL5). These molecules exert their effects through activation of CC-chemokine receptor 5 (CCR5).⁴ CCR5 is expressed at low levels in the normal brain, but it can be induced to play important roles in various injuries or infections, including AD.⁵ In this context, immunohistochemical analyses have revealed the expression of CCR5, together with its ligands, on the microglia of both normal and AD brains, with increased expression on some reactive microglia in AD.¹¹ Nevertheless, the precise role of CCR5 and its ligand MIP-1 α in AD is poorly understood so far.

In the current study we have investigated the molecular and behavioral alterations induced by a single intracerebroventricular (i.c.v.) injection of $A\beta_{1-40}$ peptide in mice lacking MIP-1 α or CCR5. Although unable to induce pathological AD hallmarks, the acute injection of $A\beta$ peptides into the rodent brain is a useful experimental model for the characterization of $A\beta$ toxicity, as it induces an inflammatory response associated with deficits of learning and memory.¹⁶ Using this model, we demonstrated that activation of the MIP-1 α /CCR5 signaling pathway is one of the earliest events after $A\beta_{1-40}$ injection in mice, representing an important signal for the accumulation of activated glial cells and, consequently, for inflammatory response, synaptic dysfunction, and cognitive failure. These findings raise the possibility that MIP-1 α and CCR5 represent promising targets for AD drug development.

Materials and Methods

Animals

Experiments were conducted using male C57BL/6 CCR5 knockout (CCR5^{-/-}) and MIP-1 α knockout (MIP-1 α ^{-/-}) mice (20 to 30 g). They were kept in controlled room temperature (22 \pm 2°C) and humidity (55 to 60%) under a 12 hour light/dark cycle (lights on at 6:00 AM). CCR5^{-/-}¹⁷ and MIP-1 α ^{-/-}¹⁸ mice are on the C57BL/6 background, constructed as described previously. All procedures used in the present study followed the *Guide for the Care and Use of Laboratory Animals* (NIH publication No. 85-23) and were approved by the Animal Ethics Committee of the Universidade Federal de Santa Catarina.

Drug Treatment Protocol

Human $A\beta_{1-40}$ (Tocris, Ellisville, MO) and the inverse peptide $A\beta_{40-1}$ (Bachem, Torrance, CA) were prepared as stock solutions at a concentration of 1 mg/ml in sterile 0.1 mol/L PBS (pH 7.4), and aliquots were stored at -20°C. $A\beta$ solutions were aggregated by incubation at 37°C for 4 days before use as described previously.¹⁹ The aggregation and/or oligomerization state of $A\beta$ solutions was confirmed through Western blot analysis (data not shown).

The aggregated form of $A\beta$ fragments (400 pmol/mice) or PBS (vehicle) was administered i.c.v. as described previously.^{20–22} In brief, the animals were anesthetized with isoflurane (2.5%, Abbott Laboratórios do Brasil Ltda., Rio de Janeiro, RJ, Brazil) using a vaporizer system (SurgiVet Inc., Waukesha, WI) and then gently restrained by hand for i.c.v. injections. The injection site was sterilized using gauze embedded in 70% ethanol. Under light anesthesia (ie, just that necessary for loss of the postural reflex), the needle was inserted unilaterally 1 mm to the right of the midline point equidistant from each eye and 1 mm posterior to a line drawn through the anterior base of the eyes (used as external reference). A volume of 3 μ l of $A\beta_{1-40}$, $A\beta_{40-1}$, or PBS solution was injected into the lateral ventricle, at the following coordinates from bregma: anteroposterior -0.22 mm, mediolateral 1 mm, and dorsoventral = -3 mm. The accurate placement of the injection site (needle track) was confirmed at the moment of dissection of the animals for molecular biology experiments. The administration site was also confirmed in parallel experiments performed by the same technician in which 2 μ l of Evans blue dye 0.5% was injected, and the brains were examined microscopically to verify the staining in the walls of the lateral ventricle (more details in Ref.²²). Results from mice presenting misplacement of the cannula or any sign of cerebral hemorrhage were excluded from the statistical analysis (overall, less than 5% of the total animals used).

To confirm the involvement of CCR5 in the glial cell accumulation induced by $A\beta_{1-40}$ i.c.v. injection, some mice were treated with the CCR5 antagonist D-Ala-peptide T-amide (0.01 mg/kg/day s.c., Tocris) administered 1 hour before $A\beta_{1-40}$ i.c.v. injection and throughout consecutive days until the day of the experiment.

Tissue Collection

For RT-PCR and Western blot experiments, the animals were sacrificed by decapitation, and the skin was removed from the skull with two forceps. Then, one blade of a pair of fine scissors was introduced into the foramen magnum, and the skull was opened by cutting along its caudal to rostral axis. Two cuts were made perpendicular to the first one, with the scissors pointing toward the left and right ears, respectively. The opening of the skull was carefully enlarged with fine forceps. The brain was removed from the skull by means of a spatula, and the brainstem was separated from the cortex. In the next step, the hippocampuses were rapidly dissected on dry ice and stored at -70°C.

For immunohistochemical studies, mice were anesthetized with chloral hydrate (400 mg/kg i.p.) and perfused transcardially with heparin (1000 U/ml) in physiological saline followed by 4% paraformaldehyde in physiological saline. The brains were rapidly removed and postfixed overnight at 4°C in 4% paraformaldehyde.

RNA Preparation and RT-PCR

Total RNA was extracted from the hippocampus using TRIzol reagent (Invitrogen, São Paulo, SP, Brazil) according to the manufacturer's instructions. Two micrograms of total RNA was reverse transcribed using oligo(dT) as a primer (0.05 μ g), 50 U of reverse transcriptase (Promega, Madison, WI), dNTP (144 μ mol/L, Promega), reaction buffer (10 mmol/L dithiothreitol, 3 mmol/L $MgCl_2$, 75 mmol/L KCl, and 50 mmol/L Tris-HCl, pH 8.3), and 2 U of RNasin Plus (Promega) in a final volume of 12.5 μ l. The cDNA was obtained after incubation of the samples at 70°C for 5 minutes, 4°C for 5 minutes, 37°C for 60 minutes, 70°C for 5 minutes, and 4°C for 5 minutes. Specific primers were used for CCR5 (sense, 5'-GCCAGAGGAGGTGAGACATC-3'; antisense, 5'-AAGAGCAGGTCA-GAGATGGC-3'), MIP-1 α (sense, 5'-ATGAAGGTCTCCAC-CACTG-3'; antisense, 5'-GCATTCAGTCCAGTCA-3'), and β -actin (sense, 5'-TCCTTCGTTGCCGGTCCACA-3'; antisense, 5'-CGTCTCCGGAGTCCATCACA-3'). β -Actin cDNA was used for standardization of the amount of RNA. Two microliters of RT aliquots was mixed in a buffer containing 10 mmol/L Tris-HCl, pH 9, 1 mmol/L $MgCl_2$, 200 μ mol/L dNTP, 300 nmol/L of each primer, and 5 U of Taq polymerase (Ludwig Biotech, Porto Alegre, RS, Brazil) in a final volume of 30 μ l. The PCR cycling protocols were as follows: initial denaturation at 95°C for 4 minutes; cycling at 95°C for 30 seconds, 54°C for 30 seconds (CCR5 and MIP-1 α), or 62°C for 30 seconds (β -actin), and 72°C for 1 minute; and a final extension period at 72°C for 5 minutes. Optimal amplification was achieved at 30 cycles. Aliquots of 5 μ l of each sample were analyzed by polyacrylamide gel electrophoresis and stained with silver nitrate. Band density measurements for CCR5, MIP-1 α , and β -actin mRNAs were made using ImageJ 1.36b imaging software (NIH, Bethesda, MD).

Western Blot

Tissues were homogenized in ice-cold 10 mmol/L HEPES (pH 7.4), containing 1.5 mmol/L $MgCl_2$, 10 mmol/L KCl, 1 mmol/L phenylmethylsulfonyl fluoride, 5 μ g/ml leupeptin, 5 μ g/ml pepstatin A, 10 μ g/ml aprotinin, 1 mmol/L sodium orthovanadate, 10 mmol/L β -glycerophosphate, 50 mmol/L sodium fluoride, and 0.5 mmol/L dithiothreitol (all from Sigma-Aldrich, St. Louis, MO). The homogenates were chilled on ice for 15 minutes, vigorously shaken for 15 minutes in the presence of 0.1% Triton X-100 and then centrifuged at 10,000 $\times g$ for 30 minutes. The supernatant containing the cytosolic fraction was stored at -70°C until use. Protein concentration was determined using a Bio-Rad protein assay kit (Bio-Rad, Hercules, CA).

Equal amounts of protein were separated by SDS-polyacrylamide gel electrophoresis and then were transferred to a polyvinylidene fluoride membrane (Immobilon P, Millipore, Danvers, MA). The membranes were saturated by incubation with 10% nonfat dry milk solution and then incubated overnight with inducible nitric oxide synthase (iNOS) (1:1000), cyclooxygenase (COX)-2 (1:1000), or β -actin (1:5000) antibody (Santa Cruz Biotech. Inc., Santa Cruz, CA). After washing, the membranes were incubated with adjusted secondary antibody coupled to horseradish peroxidase. The immunocomplexes were visualized using the an ECL chemiluminescence detection system (GE Healthcare, São Paulo, SP, Brazil). Band density measurements were made using ImageJ 1.36b.

Immunohistochemistry

Immunohistochemical analysis was performed on paraffin-embedded brain tissue sections using CD68 (1:100, Abcam, Cambridge, MA), synaptophysin (1:400, Novocastra, Newcastle, UK), glial fibrillary acid protein (GFAP) (1:600), phospho (p)-p65 nuclear factor- κ B (NF- κ B; 1:100), p-cAMP-response element-binding (CREB; 1:200), p-c-Jun/activator protein-1 (AP-1) (1:300), or COX-2 (1:200) antibodies (Cell Signaling Technology, Danvers, MA). After quenching of endogenous peroxidase with 1.5% hydrogen peroxide in methanol (v/v) for 20 minutes, high-temperature antigen retrieval was performed by immersion of the slides in a water bath at 95 to 98°C in 10 mmol/L trisodium citrate buffer, pH 6.0, for 45 minutes. The slides were then processed using the Vectastain Elite ABC reagent (Vector Laboratories, Burlingame, CA) according to the manufacturer's instructions. After the appropriate biotinylated secondary antibody, sections were developed with 3,3'-diaminobenzidine (Dako Cytomation, Glostrup, Denmark) in chromogen solution for the exact amount of time and counterstained with Harris's hematoxylin. Control and experimental tissues were placed on the same slide and processed under the same conditions.

The immunostaining was assessed at four levels of the dorsal hippocampus. Specifically, four alternate 3- μ m sections of the hippocampus with an individual distance of ~150 μ m were obtained between 1.6 and 2.4 mm posterior to the bregma. Images of stained hippocampal CA1, CA2, and CA3 and dentate gyrus subregions were acquired using a Sight DS-5M-L1 digital camera (Nikon, Melville, NY) connected to an Eclipse 50i light microscope (Nikon). A threshold optical density that best discriminated staining from the background was obtained using the ImageJ 1.36b. We captured two images of each hippocampal subregion per section (8 images per section and 32 images per mouse).

For p-CREB or COX-2 burden analyses, data are reported as the percentage of labeled area captured (positive pixels) divided by the full area captured (total pixels), as described previously.²³ For synaptophysin analysis, total pixel intensity was determined, and data were expressed as optical density. The data represent the average value obtained by the analysis of images of the hippocampal CA1, CA2, and CA3 and dentate gyrus subregions.

The numbers of CD68, GFAP, p-p65 NF- κ B, or p-c-Jun AP-1 stained-positive cells were examined microscopically at $\times 40$ magnification. The numbers of stained-positive cells within the CA1, CA2, CA3, and dentate gyrus subregions of each of the four 3- μ m sections were counted. The mean number of stained-positive cells per section was calculated for each animal group.

All histological assessments were made by an examiner blinded to sample identities. Some inherent weaknesses of the two-dimensional counting and densitometry methods applied in this study have been reviewed elsewhere.²⁴

Immunofluorescence

For the immunofluorescence experiments, brains were sectioned at 40 μ m using a Vibratome (Pelco, Redding, CA). Sections were first blocked with 3% normal serum with 2% bovine serum albumin and 0.1% Triton X-100 in Tris-buffered saline and then were incubated with ionized calcium binding adaptor molecule-1 (Iba-1) primary antibody (1:200) (Wako Chemicals, Richmond, VA) in blocking solution overnight at 4°C. Sections were then rinsed and incubated for 1 hour with secondary Alexa Fluor-conjugated antibody (Invitrogen) at room temperature. Finally, sections were mounted onto gelatin-coated slides in Fluoromount-G (Southern Biotech, Birmingham, AL) and examined under a confocal laser microscope (Olympus, Tokyo, Japan) using Laser Sharp 2000 software (Bio-Rad). The number of Iba-1-positive cells was examined microscopically at $\times 40$ magnification at four levels of the dorsal hippocampus with an individual distance of ~ 150 μ m, obtained between 1.6 and 2.4 mm posterior to the bregma. The numbers of stained-positive cells within the CA1, CA2, CA3, and dentate gyrus subregions of each of the four sections were counted. The mean number of stained-positive cells per section was calculated for each animal group.

Chemotaxis Assay

Resident peritoneal macrophages were harvested from wild-type (C57BL/6), CCR5^{-/-}, or MIP-1 α ^{-/-} mice. Cells were incubated on 24-well cell culture plates (10⁶ cells/well) in RPMI 1640 containing 5% fetal calf serum, 2 mmol/L L-glutamine, 150 U/ml penicillin, and 150 μ g/ml streptomycin (Invitrogen) at 37°C and were stimulated with A β ₁₋₄₀ or A β ₄₀₋₁ (30 μ mol/L). After 24 hours the supernatant was harvested and stored at -80°C. The chemotaxis assays were performed with a chemotaxis instrument (Neuro Probe, Inc., Gaithersburg, MD). In brief, 27 μ l of supernatant from wild-type, CCR5^{-/-}, or MIP-1 α ^{-/-} macrophages, stimulated with A β ₁₋₄₀ or A β ₄₀₋₁, was placed in the lower compartment of the chemotaxis chamber, and 50 μ l of 3 \times 10⁶ cells/ml (obtained from wild-type, CCR5^{-/-}, or MIP-1 α ^{-/-} mice) was placed in the upper compartment. The two compartments were separated by a porous polycarbonate filter (5- μ m pore size). Macrophages were allowed to migrate for 2 hours at 37°C, and the number of cells that had

migrated to the lower surface of the filter was determined using a light microscope. The cells were counted in the May-Grünwald-Giemsa-stained filters under oil immersion magnification in 20 consecutive noncoincident fields. The chemotaxis index represents the number of cells that migrated in response to supernatant from stimulated macrophages divided by the number of cells that migrated in response to supernatant from unstimulated macrophages. Each data point is the result of triplicate measurements, from a single representative experiment. Each experiment was repeated three times with similar results.

Tumor Necrosis Factor- α and Interleukin-1 β Enzyme-Linked Immunosorbent Assay and Cell Viability

Resident peritoneal macrophages were obtained from wild-type, CCR5^{-/-}, or MIP-1 α ^{-/-} mice and were stimulated with A β ₁₋₄₀ (30 μ mol/L), A β ₄₀₋₁ (30 μ mol/L), *Escherichia coli* lipopolysaccharide (LPS) (serotype 0111:B4, 100 ng/ml, Sigma-Aldrich), or complement component C5a (10 nmol/L, Sigma-Aldrich) for 24 hours. The levels of tumor necrosis factor- α (TNF- α) and interleukin-1 β (IL-1 β) in supernatants were measured using commercially available enzyme-linked immunosorbent assay kits (R&D Systems, Minneapolis, MN). The cell viability of the stimulated macrophages was determined by mitochondrial-dependent reduction of 3-(4,5-dimethylthiazol-2-yl)-2,5-diphenyltetrazolium bromide (Sigma-Aldrich) to formazan as described previously.²⁵

Water Maze

The Morris water maze test was performed as described previously.²⁶ The experimental apparatus consisted of a circular tank (diameter 97 cm; height 60 cm) containing water at 22 \pm 2°C. The target platform (10 \times 10 cm) was submerged 1 cm below the surface and placed at the midpoint of one quadrant. The platform was located in a fixed position, equidistant from the center and the wall of the tank. The tank was located in a test room containing various prominent visual cues. Mice were submitted to a spatial reference memory version of the water maze as described previously.²⁰⁻²² The acquisition training session was performed 7 days after A β ₁₋₄₀ injection and consisted of 10 consecutive trials, during which the animals were left in the tank facing the wall and allowed to swim freely to the escape platform. If an animal did not find the platform within a period of 60 seconds, it was gently guided to it. The animal was allowed to remain on the platform for 10 seconds after escaping to it and was then removed from the tank for 5 minutes before being placed at the next starting point in the tank. This procedure was repeated 10 times, with the starting points varying in a pseudo-randomized manner. The test session was performed 24 hours after the training session (on day 8 postinjection). The test session consisted of a single probe trial in which the platform was removed from

the tank and each mouse was allowed to swim for 60 seconds in the maze. Performance was monitored with an AnyMaze video-tracking system (Stoelting Co., Wood Dale, IL).

Open Field

To evaluate the possible effects of MIP-1 α or CCR5 genetic deletion and/or A β ₁₋₄₀ administration on locomotor activity, the animals were tested in the open-field paradigm. The apparatus, made of wood covered with impermeable Formica, had a black floor of 30 × 30 cm (divided by white lines into nine squares of 10 × 10 cm) and transparent walls, 15 cm high. Each mouse was placed in the center of the open field, and the total number of squares crossed with the four paws and the rearing behavior were registered for 5 minutes.

Statistical Analysis

All data are expressed as mean ± SEM. Statistical evaluation of the results was performed using appropriate analysis of variance with genotype, treatment, time, or the number of trials (repeated measures) as independent variables. After significant analyses of variance, multiple post hoc comparisons were performed using the Bonferroni test. The accepted level of significance for the tests was *P* < 0.05. All tests were performed using the Statistica software package (StatSoft Inc., Tulsa, OK).

Results

A β ₁₋₄₀ Induces Up-Regulation of MIP-1 α and Glial Cell Activation in Mouse Hippocampus

The expression of the mRNAs for MIP-1 α and CCR5 was assessed in the hippocampuses of wild-type mice at different time points after A β ₁₋₄₀ i.c.v. treatment by means of RT-PCR. Under basal conditions, very low levels of hippocampal MIP-1 α mRNA were observed. Conversely, a rapid onset and time-dependent induction of MIP-1 α mRNA was found in A β ₁₋₄₀-treated mice (Figure 1, A and C). A significant increase in MIP-1 α mRNA levels was detected after 1 hour of A β ₁₋₄₀ treatment, reaching a peak at 24 hours, and remaining elevated for up to 8 days. Moreover, the time course analysis revealed that the CCR5 mRNA level was not significantly affected by A β ₁₋₄₀ treatment (Figure 1, B and D). In addition, the treatment of animals with the reverse peptide A β ₄₀₋₁ had no effect on the MIP-1 α or CCR5 mRNA levels (Supplemental Figure S1, see <http://ajp.amjpathol.org>).

To assess whether this increase in MIP-1 α levels was associated with the accumulation of activated astrocytes and microglia, we evaluated the number of GFAP- and CD68-positive cells in the hippocampus, respectively. The results in Figure 1, E and F, demonstrate that a striking elevation in the number of GFAP-positive cells occurred between 6 hours and 8 days after A β ₁₋₄₀ treatment compared with the number in naive animals. Like-

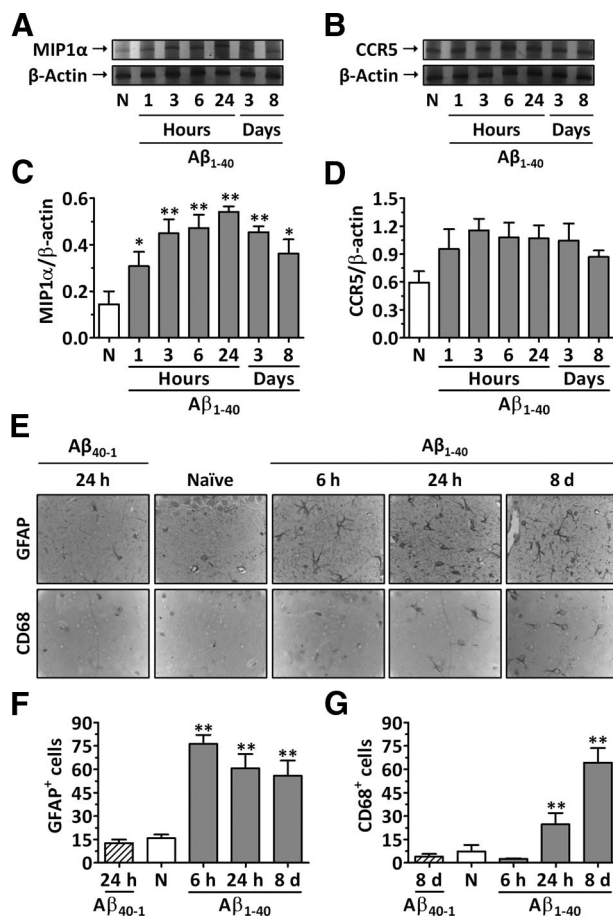


Figure 1. Effect of A β ₁₋₄₀ on the expression of MIP-1 α and CCR5 and in glial cell activation in mouse hippocampus. Wild-type C57BL/6 mice were left untreated (naive mice, N) or were treated i.c.v. with A β ₁₋₄₀ or A β ₄₀₋₁ (400 pmol/mouse), and brains were harvested at the time points indicated. Total RNA was isolated from hippocampuses for evaluation of MIP-1 α and CCR5 mRNA expression, and β -actin mRNA was assessed as an internal control for the amount of RNA in each sample. Representative RT-PCR analysis showing MIP-1 α (A) and CCR5 mRNA (B) expression. Densitometric analysis is expressed as the MIP-1 α / β -actin (C) and the CCR5/ β -actin ratio (D). E: Representative images of GFAP and CD68 immunostaining in the CA1 subregion of the hippocampus. Original magnification, ×100. Graphic representation of the number of GFAP- (F) and CD68-positive cells (G) determined in the CA1, CA2, CA3, and dentate gyrus subregions of the hippocampus. The values represent the mean ± SEM (*N* = 3 to 5 mice/group). **P* < 0.05 and ***P* < 0.01 compared with the naive group.

wise, a significant increase in the number of CD68-positive cells was found 1 day after A β ₁₋₄₀ administration, reaching a peak at day 8 after treatment (Figure 1, E and G). In addition, treatment of animals with the reverse peptide A β ₄₀₋₁ had no effect on the number of GFAP- or CD68-positive cells when evaluated 24 hours after the treatment (Figure 1, E-G).

Effect of Genetic Deletion of MIP-1 α or CCR5 in A β ₁₋₄₀-Induced Glial Cell Activation in Mouse Hippocampus

Glial cell activation is one of the earliest pathological features of AD and may occur in response to the increasing number of degenerating neurons and synapses or to the accumulation of A β . The data in Figure 2, A and C

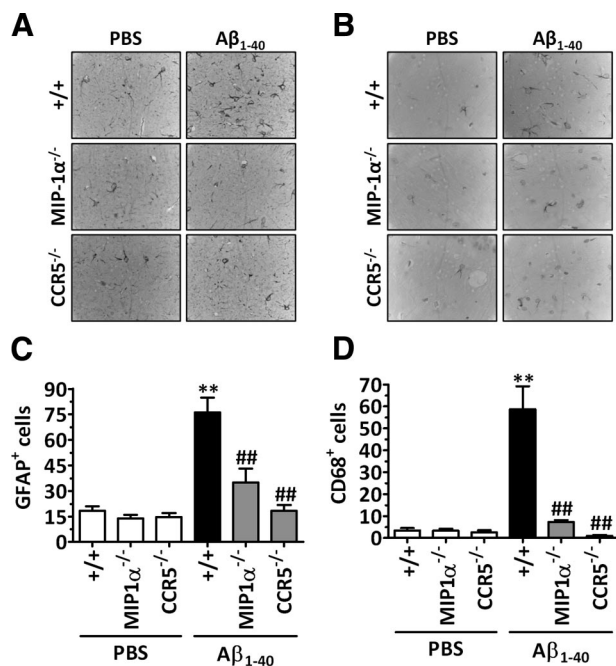


Figure 2. Involvement of MIP-1 α and CCR5 in A β_{1-40} -induced glial cell activation in mouse hippocampus. Immunohistochemical analysis for GFAP and CD68 was performed 6 hours or 8 days after A β_{1-40} (400 pmol/mouse) or PBS i.c.v. injection, respectively. Mice lacking MIP-1 α or CCR5 showed a reduced number of GFAP- (A and C) and CD68-positive cells (B and D) in the hippocampus. Representative images of GFAP (A) and CD68 immunostaining (B) in the CA1 subregion of the hippocampus. Original magnification, $\times 100$. Graphic representation of the number of GFAP- (C) and CD68-positive cells (D) determined in the CA1, CA2, CA3, and dentate gyrus subregions of the hippocampus. The values represent the mean \pm SEM ($N = 5$ mice/group). ** $P < 0.01$ compared with the PBS-treated wild-type mouse group. ## $P < 0.01$ compared with the A β_{1-40} -treated wild-type mouse group.

indicate that, in comparison with wild-type mice, the genetic deletion of CCR5 or its ligand MIP-1 α resulted in a significant reduction in the number of activated astrocytes in the hippocampus when evaluated 6 hours after A β_{1-40} administration, as demonstrated by a reduction in the number of GFAP-positive cells. Likewise, when evaluated 8 days after A β_{1-40} treatment, mice lacking MIP-1 α or CCR5 showed a reduced number of CD68-positive cells that was comparable with that observed in the hippocampuses of PBS-treated mice, indicating a diminished number of activated microglial cells (Figure 2, B and D). Of note, it was not possible to observe differences in brain size or morphology between MIP-1 α - or CCR5-deficient mice and their wild-type littermates, and immunohistochemical analysis failed to reveal any alteration in glial cell activation among the different mouse genotypes treated with PBS.

To confirm the involvement of CCR5 in glial cell accumulation induced by A β_{1-40} treatment, the number of Iba-1-positive cells was evaluated in the hippocampuses of CCR5 antagonist D-Ala-peptide T-amide-treated mice (Supplemental Figure S2, see <http://ajp.amjpathol.org>). A significant increase in the number of Iba-1-positive cells was observed as early as 24 hours and persisted until at least 8 days after A β_{1-40} injection. In addition, pharmacological treatment with D-Ala-peptide T-amide (0.01 mg/kg/day s.c.) significantly reduced the increase in the number of Iba-1-positive

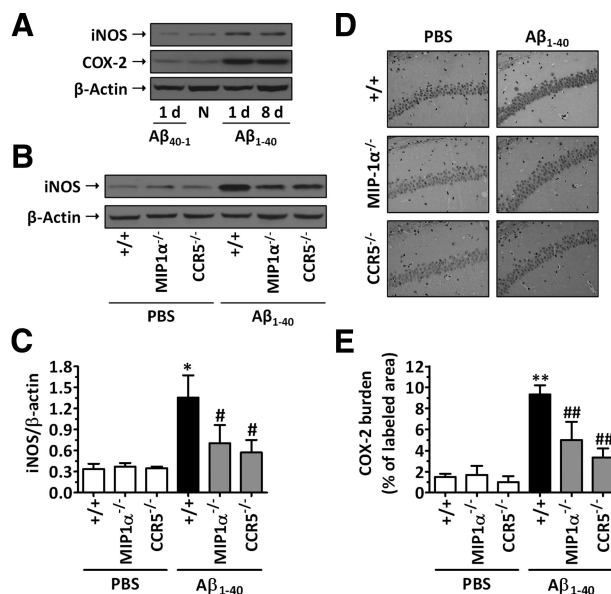


Figure 3. MIP-1 α and CCR5 modulate A β_{1-40} -induced iNOS and COX-2 up-regulation. **A:** A β_{1-40} induced time-dependent iNOS and COX-2 protein expression in the hippocampus. Western blot analysis for iNOS, COX-2, and β -actin (loading control) was performed in the hippocampuses of wild-type C57BL/6 mice 1 and 8 days after A β_{1-40} (400 pmol/mouse) i.c.v. injection. Some mice were left untreated (naive mice, N) or were treated with the reverse A β_{40-1} peptide (400 pmol/mouse i.c.v.). **B:** MIP-1 α and CCR5 genetic deletion resulted in a reduction of iNOS up-regulation induced by A β_{1-40} , when evaluated 1 day after treatment. **C:** Graph showing quantification of iNOS protein normalized by β -actin protein (loading control). For COX-2 protein, immunohistochemical analysis was performed 1 day after A β_{1-40} (400 pmol/mouse) or PBS i.c.v. injection. **D:** Representative images of COX-2 immunostaining, demonstrating diminished levels of this enzyme in the CA1 hippocampal subregion of MIP-1 α ^{-/-} and CCR5^{-/-} mice. Original magnification, $\times 40$. **E:** Graphic representation of the average immunostaining for COX-2 evaluated in the CA1, CA2, CA3, and dentate gyrus subregions of the hippocampus. The values represent the mean \pm SEM ($N = 6$ to 7 mice/group). * $P < 0.05$ and ** $P < 0.01$ compared with the PBS-treated wild-type mouse group. # $P < 0.05$ and ## $P < 0.01$ compared with the A β_{1-40} -treated wild-type mouse group.

cells induced by A β_{1-40} in the hippocampus (Supplemental Figure S2, see <http://ajp.amjpathol.org>).

MIP-1 α and CCR5 Are Required for A β_{1-40} -Induced Inflammatory Response in Mouse Hippocampus

The expression of the enzymes iNOS and COX-2 in the hippocampuses of mice was assessed 1 and 8 days after i.c.v. injection of A β peptides. The data in Figure 3A indicate that the injection of A β_{1-40} , but not of A β_{40-1} , resulted in a marked induction of both iNOS and COX-2 up-regulation in wild-type mice, reaching a peak at 1 day and lasting for up to 8 days after treatment. Western blot analysis revealed that genetic deletion of MIP-1 α or CCR5 attenuated A β_{1-40} -induced iNOS up-regulation, when evaluated 1 day after administration (inhibition of 47 and 68%, respectively) (Figure 3, B and C). In addition, COX-2 up-regulation induced by A β_{1-40} was found to be significantly diminished in both MIP-1 α ^{-/-} and CCR5^{-/-} mice at 1 day compared with that in wild-type A β_{1-40} -treated mice, as indicated by reduced immunostaining for COX-2 (inhibition of 50 and 70%, respectively) (Figure

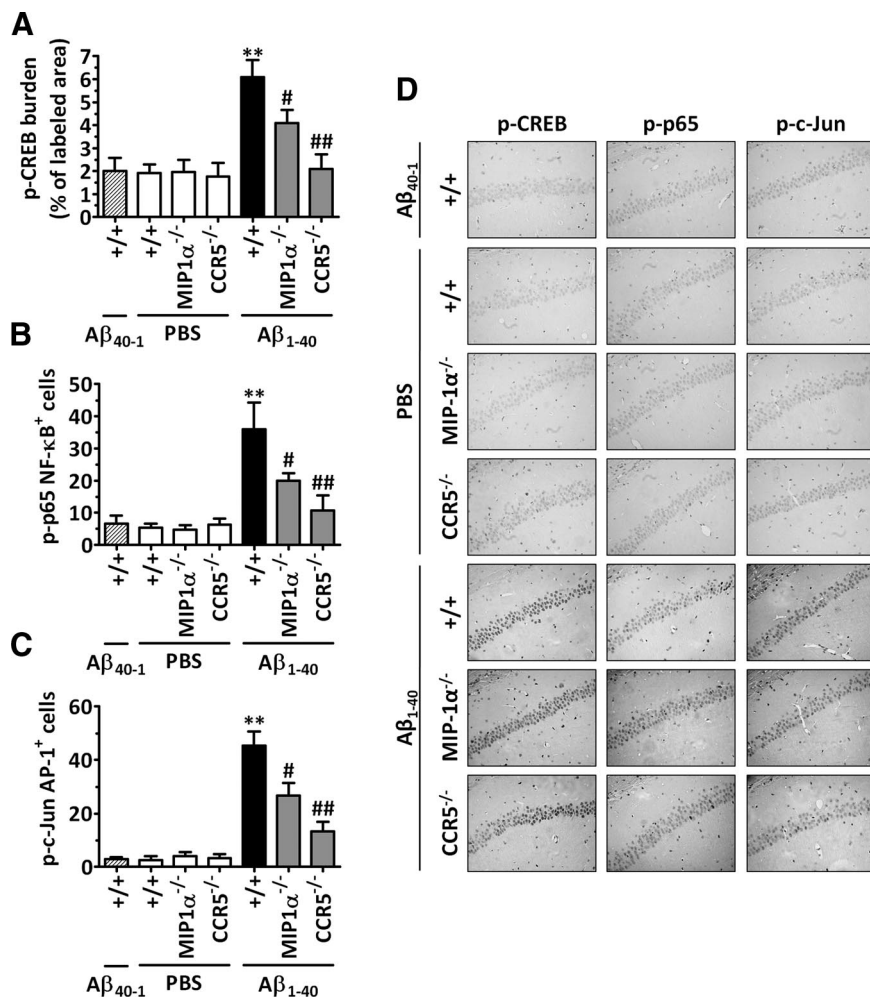


Figure 4. Role of MIP-1 α and CCR5 in intracellular pathways activated in response to A β_{1-40} . Immunohistochemical analysis for p-CREB, p-p65 NF- κ B, and p-c-Jun/AP-1 protein was performed 6 hours after A β_{1-40} (400 pmol/mouse), A β_{40-1} (400 pmol/mouse), or PBS i.c.v. injection. **A:** Graphic representation of the average immunostaining for p-CREB, demonstrating reduced activation in the CA1, CA2, CA3, and dentate gyrus subregions of the hippocampus of MIP-1 $\alpha^{-/-}$ and CCR5 $^{-/-}$ mice. Similar results were observed when the number of positive cells for p-p65 NF- κ B (**B**) and p-c-Jun AP-1 (**C**) per section was determined. The values represent the mean \pm SEM ($N = 5$ mice/group). ** $P < 0.01$ compared with the PBS-treated wild-type mouse group. * $P < 0.05$ and ** $P < 0.01$ compared with the A β_{1-40} -treated wild-type mouse group. **D:** Representative images of nuclear p-CREB, p-p65 NF- κ B, and p-c-Jun AP-1 immunostaining in the CA1 hippocampal subregion of wild-type, MIP-1 $\alpha^{-/-}$, and CCR5 $^{-/-}$ mice. Original magnification, $\times 40$.

3, D and E). Notably, no significant alteration in iNOS and COX-2 expression could be observed in MIP-1 $\alpha^{-/-}$ and CCR5 $^{-/-}$ PBS-treated mice compared with wild-type PBS-treated mice.

Role of MIP-1 α and CCR5 in A β_{1-40} -Induced Transcription Factor Activation

It has been reported previously that CCR5 is involved in the activation of transcription factors in the hippocampus during inflammation.²⁷ In addition, the production of COX-2 and iNOS proteins is tightly regulated at the transcriptional level.^{28,29} Thus, we attempted to evaluate the effects of MIP-1 α and CCR5 in the A β_{1-40} -induced activation of transcription factors established in the 5'-flanking region of the COX-2 and iNOS gene promoter. Basal activation of CREB, p65 NF- κ B, and c-Jun/AP-1 can be found in the hippocampus of wild-type, MIP-1 $\alpha^{-/-}$, and CCR5 $^{-/-}$ mice. In accordance with our previous reports,²⁰ A β_{1-40} i.c.v. injection resulted in a significant activation of these transcription factors in the wild-type mouse hippocampus, as indicated by the increase in the CREB, p65 NF- κ B, and c-Jun/AP-1 phosphorylated levels 6 hours after treatment. Conversely, MIP-1 α or CCR5 genetic deletion significantly inhibited the increase in

A β_{1-40} -induced transcriptional activity (Figure 4, A–D). The phosphorylated levels of CREB, p65 NF- κ B, and c-Jun/AP-1 found in the MIP-1 $\alpha^{-/-}$ A β_{1-40} -treated mice were reduced by 45, 50, and 43%, respectively, in comparison with those in the wild-type A β_{1-40} -treated mice. Likewise, mice lacking CCR5 showed a striking inhibition of A β_{1-40} -induced CREB, p65 NF- κ B, and c-Jun/AP-1 activation, with phosphorylation levels similar to those observed in PBS-treated mice (inhibitions of 94, 80, and 80%, respectively).

Requirement of MIP-1 α and CCR5 to A β_{1-40} -Induced Cellular Responses in Vitro

To confirm the involvement of MIP-1 α and CCR5 in the regulation of cellular migration, as well as in the activation of the inflammatory response induced by A β_{1-40} , we performed a series of *in vitro* experiments using peritoneal macrophages obtained from wild-type, MIP-1 $\alpha^{-/-}$, or CCR5 $^{-/-}$ mice. Initially, a chemotaxis assay was performed using as chemotactic stimulus the supernatant obtained from cultured macrophages isolated from wild-type, MIP-1 $\alpha^{-/-}$, or CCR5 $^{-/-}$ mice, stimulated for 24 hours with A β_{1-40} or with the reverse peptide A β_{40-1} . The results in Figure 5A demonstrate no alteration in the mi-

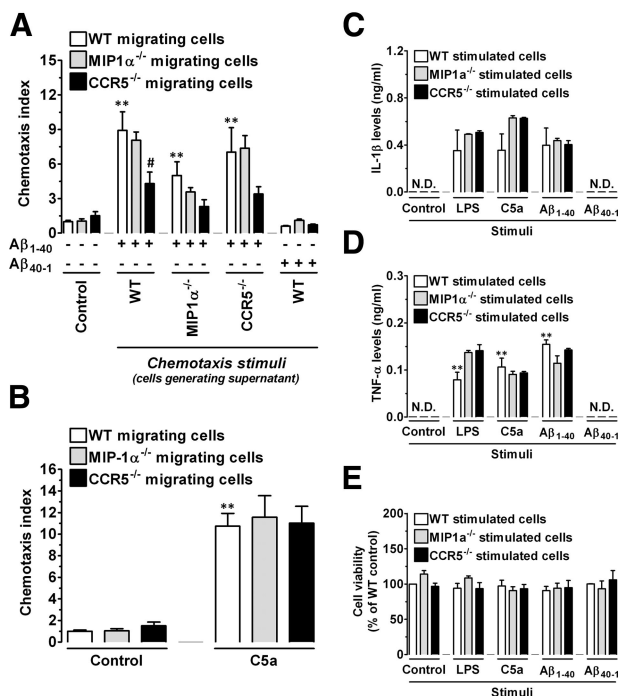


Figure 5. MIP-1 α and CCR5 are required for cellular migration but not for activation induced by $A\beta_{1-40}$ *in vitro*. Peritoneal macrophages were isolated from wild-type (WT), MIP-1 $\alpha^{-/-}$, or CCR5 $^{-/-}$ mice, cultured on 24-well plates, and incubated with 30 μ mol/L $A\beta_{1-40}$ or $A\beta_{40-1}$ for 24 hours, and the supernatant was collected and assayed for chemotactic activity. Chemotaxis of wild-type, MIP-1 $\alpha^{-/-}$, and CCR5 $^{-/-}$ macrophages in response to the supernatants was assayed using the Neuro Probe transwell assay. Chemotactic index represents the number of cells that migrated in response to supernatant from stimulated macrophages/number of cells that migrated in response to supernatant from unstimulated macrophages. **A:** MIP-1 $\alpha^{-/-}$ macrophages produce reduced chemotactic activity for wild-type, MIP-1 $\alpha^{-/-}$, and CCR5 $^{-/-}$ cells when stimulated with $A\beta_{1-40}$ compared with wild-type and CCR5 $^{-/-}$ macrophages. Macrophages isolated from CCR5 $^{-/-}$ mice show a diminished chemotactic index in response to supernatant of $A\beta_{1-40}$ -stimulated wild-type, MIP-1 $\alpha^{-/-}$, or CCR5 $^{-/-}$ cells. No significant chemotactic activity for macrophages was induced in response to the $A\beta_{40-1}$. **B:** Macrophage chemotaxis toward C5a (100 ng/ml) was not affected by genetic deletion of MIP-1 α or CCR5. IL-1 β (**C**) or TNF- α (**D**) released into the supernatant of macrophages of wild-type, MIP-1 $\alpha^{-/-}$, and CCR5 $^{-/-}$ mice stimulated for 24 hours with 30 μ mol/L $A\beta_{1-40}$ or $A\beta_{40-1}$, LPS (100 ng/ml), or C5a (10 nmol/L) was measured by enzyme-linked immunosorbent assay. **E:** Cell viability assessed after stimulation with $A\beta_{1-40}$, $A\beta_{40-1}$, LPS, or C5a. "Control" refers to unstimulated cells. Values represent the mean \pm SEM ($N=3$ /group). Chemotaxis assays were performed in triplicate, and ELISA experiments in duplicate. ** $P < 0.01$ compared with the control group. * $P < 0.05$ compared with the $A\beta_{1-40}$ -treated wild-type group. N.D., not determined.

gration of cells isolated from wild-type, MIP-1 $\alpha^{-/-}$, or CCR5 $^{-/-}$ mice in response to supernatant from cultured cells stimulated with $A\beta_{40-1}$ compared with unstimulated cells (control). We found that in contrast to wild-type or MIP-1 $\alpha^{-/-}$ macrophages, CCR5 $^{-/-}$ macrophages showed reduced migration toward the supernatant of macrophages obtained from wild-type or CCR5 $^{-/-}$ mice stimulated with $A\beta_{1-40}$. Furthermore, the supernatant of $A\beta_{1-40}$ -stimulated MIP-1 $\alpha^{-/-}$ macrophages was less effective in inducing the migration of cells obtained from wild-type, MIP-1 $\alpha^{-/-}$, or CCR5 $^{-/-}$ mice, in comparison with the supernatant of $A\beta_{1-40}$ -stimulated wild-type macrophages. Importantly, wild-type, MIP-1 $\alpha^{-/-}$, and CCR5 $^{-/-}$ macrophages migrated equally toward another chemotactic stimulus, the complement anaphylatoxin C5a (Figure 5B). To determine whether MIP-1 $\alpha^{-/-}$ or

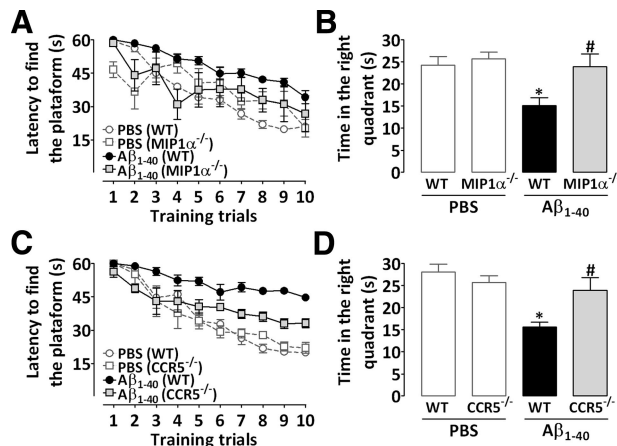


Figure 6. Contribution of MIP-1 α and CCR5 to cognitive deficits induced by $A\beta_{1-40}$ in mice. The spatial reference memory version of the Morris water maze test was used as a measure of cognition. Training trials were performed on day 7 after a single i.c.v. administration of $A\beta_{1-40}$ (400 pmol/mouse) or vehicle (PBS). Data are presented as means \pm SEM latency (seconds) for escape to a hidden platform ($n=8-10$ mice/group). The probe test session was performed 24 hours after training trials. Data are presented as means \pm SEM of the frequency of time spent in the correct quadrant. MIP-1 $\alpha^{-/-}$ (**A** and **B**) and CCR5 $^{-/-}$ (**C** and **D**) mice were significantly more resistant than wild-type (WT) C57Bl/6 mice to the deleterious effect of $A\beta_{1-40}$ in spatial learning (**A** and **C**) and spatial retrieval (**B** and **D**). * $P < 0.05$ compared with the PBS-treated wild-type mouse group; # $P < 0.05$ compared with the $A\beta_{1-40}$ -treated wild-type mouse group.

CCR5 $^{-/-}$ mononuclear phagocytes had some defect in their ability to become activated by $A\beta_{1-40}$, we used enzyme-linked immunosorbent assays to measure inflammatory cytokine production. We found that stimulation of wild-type, MIP-1 $\alpha^{-/-}$, or CCR5 $^{-/-}$ macrophages with $A\beta_{40-1}$ was not capable of stimulating the production of detectable levels of IL-1 β or TNF- α (Figure 5, C and D). Conversely, MIP-1 $\alpha^{-/-}$, CCR5 $^{-/-}$, and wild-type macrophages produced equivalent amounts of IL-1 β or TNF- α in response to $A\beta_{1-40}$ (Figure 5, C and D). A similar effect was observed when macrophages derived from different mouse genotypes were subjected to stimulation with either C5a or LPS. Notably, none of the stimuli used in these experiments reduced cell viability at the concentrations used, as demonstrated by the 3-(4,5-dimethylthiazol-2-yl)-2,5-diphenyltetrazolium bromide assay (Figure 5E). These results indicate that MIP-1 α and CCR5 directly regulate the cellular migration process but not the production of inflammatory mediators.

Effect of Genetic Deletion of MIP-1 α or CCR5 in $A\beta_{1-40}$ -Induced Learning and Memory Impairment

AD is characterized clinically by a progressive and irreversible decline in learning and memory processes. We examined the ability of mice to acquire (training session) and retrieve (test session) spatial information in the water maze paradigm as indicative of learning and memory functions. Consistent with our previous reports,²⁰⁻²² the i.c.v. administration of $A\beta_{1-40}$ (400 pmol/mouse) resulted in a marked decline in both learning and memory in wild-type mice, as indicated by longer latencies in finding

Table 1. Effects of I.C.V. Administration of $A\beta_{1-40}$ or Control Solution on Locomotor Activity of Wild-Type C57BL/6, $MIP-1\alpha^{-/-}$, or $CCR5^{-/-}$ Mice Evaluated in the Open Field (for 5 minutes)

Treatment	Mouse strain	Squares crossing	Rearing
Control (PBS)	Wild-type	101 ± 4	34 ± 2
	$MIP-1\alpha^{-/-}$	125 ± 6*	30 ± 2
	$CCR5^{-/-}$	96 ± 4*	37 ± 2
$A\beta_{1-40}$ (400 pmol/mouse)	Wild-type	102 ± 6	32 ± 2
	$MIP-1\alpha^{-/-}$	135 ± 7*	35 ± 3
	$CCR5^{-/-}$	93 ± 4*	36 ± 2

Data are expressed as the mean ± SEM of the total squares crossed and rearing. Experiments were performed on day 8 after treatments.

* $P < 0.01$ compared to the respective wild-type group.

the platform during the training session (Figure 6, A and C) and reduced target quadrant preference during the test session (Figure 6, B and D). No cognitive deficits were observed in mice treated with $A\beta_{40-1}$ (result not shown) or PBS (Figure 6). As shown in Figure 6A, genetic deletion of $MIP-1\alpha$ resulted in marked protection against $A\beta_{1-40}$ -induced spatial learning deficits, with a reduction in the final escape latency in finding the platform in the training session in comparison with wild-type mice treated with $A\beta_{1-40}$. In the test session, $MIP-1\alpha^{-/-}$ mice injected with $A\beta_{1-40}$ presented higher swimming scores in the correct quadrant compared with those for wild-type $A\beta_{1-40}$ -treated mice, indicating diminished sensitivity to learning and memory deficits induced by this peptide (Figure 6B). We next examined the role of the $CCR5$ in $A\beta_{1-40}$ -induced cognitive decline. $CCR5^{-/-}$ mice exhibited a significant decrease in the final escape latency in finding the platform during the training session (Figure 6C), as well as a significant increase in the time spent in the correct quadrant during the test session (Figure 6D) compared with wild-type mice, thus indicating a diminished sensitivity to cognitive impairment induced by $A\beta_{1-40}$ injection. Importantly, the effects of $A\beta_{1-40}$ administration on water maze performance are not directly related to motor impairment, because no significant alterations of the swimming speed and total distance traveled in the water maze were observed in wild-type, $MIP-1\alpha^{-/-}$, or $CCR5^{-/-}$ mice (results not shown). In addition, no alterations in the locomotor parameters (total squares

crossed and rearing) evaluated in the open field test were observed in $A\beta_{1-40}$ -treated mice (Table 1).

Prevention of Synaptic Dysfunction by $MIP-1\alpha$ and $CCR5$ Genetic Deletion

We had demonstrated previously²⁰ that i.c.v. injection of $A\beta_{1-40}$ evoked a significant reduction in the synaptophysin level when assessed 8 days after injection, suggesting a decrease in synaptic density. As illustrated in Figure 7, A and B, wild-type mice treated with $A\beta_{1-40}$ (400 pmol/mouse, 8 days before) exhibited markedly reduced expression of the protein synaptophysin in the hippocampus. Interestingly, both $MIP-1\alpha^{-/-}$ and $CCR5^{-/-}$ mice were more resistant to the $A\beta_{1-40}$ -induced reduction in synaptic density, as demonstrated by the significantly elevated levels of synaptophysin compared with those in wild-type $A\beta_{1-40}$ -treated mice (inhibition of 50 and 100%, respectively). Of note, no significant alteration was observed in synaptophysin levels of wild-type, $MIP-1\alpha^{-/-}$, or $CCR5^{-/-}$ mice treated with PBS or $A\beta_{40-1}$.

Discussion

Immune cell recruitment to tissue injury sites is a key step in the inflammatory process.³⁰ In AD, the initial inflammatory stimulus is thought to be the extracellular deposition of insoluble aggregates of $A\beta$ peptide. The $A\beta$ deposits lead to accumulation of activated glial cells, which in turn produce cytokines, chemokines, and neurotoxins, and, therefore, they may contribute to the neuronal degeneration observed in AD.^{15,31} However, the exact mechanisms involved in inflammatory cell accumulation observed in AD, as well as the consequences of this event, are still a matter of debate. We used an experimental model in which $A\beta_{1-40}$ was administered to mice deficient in $MIP-1\alpha$ or $CCR5$ to evaluate the role of this chemokine and its receptor in AD. The data obtained indicate a critical role for both proteins in the accumulation of activated glial cells in the hippocampus and, as a result, in the development of neuroinflammation and cognitive deficits induced by $A\beta_{1-40}$.

$MIP-1\alpha$ is one of the most commonly expressed chemokines during CNS inflammation.^{32,33} It has been re-

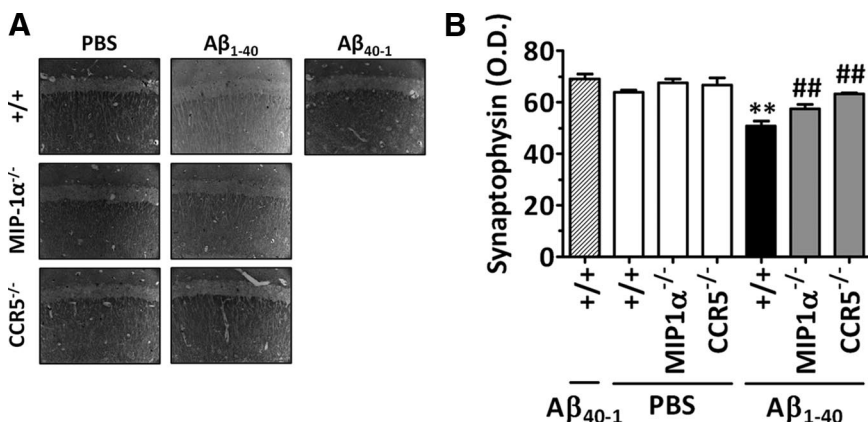


Figure 7. Role of $MIP-1\alpha$ and $CCR5$ in $A\beta_{1-40}$ -induced synaptic disruption. **A:** Representative images of synaptophysin immunostaining in the CA1 subregion of the hippocampus evaluated 8 days after PBS, $A\beta_{1-40}$, or $A\beta_{40-1}$ i.c.v. administration (400 pmol/mouse). Original magnification, $\times 40$. **B:** Graphic representation of the average optical density (O.D.) of the immunostaining for synaptophysin evaluated in the CA1, CA2, CA3, and dentate gyrus subregions of the hippocampus, demonstrating that $MIP-1\alpha^{-/-}$ and $CCR5^{-/-}$ mice were significantly more resistant than wild-type mice to $A\beta_{1-40}$ -induced synaptic disruption. The values represent the mean ± SEM ($N = 5$ mice/group). ** $P < 0.01$ compared with the PBS-treated wild-type mouse group. ## $P < 0.01$ compared with the $A\beta_{1-40}$ -treated wild-type mouse group.

ported that MIP-1 α is expressed by neurons and microglia in AD brains¹¹ and by microglia, macrophages, astrocytes, and oligodendrocytes stimulated with A β *in vitro*.^{34–38} In addition, it has been demonstrated that CCR5 is expressed by neurons, microglia, and astrocytes in the brain.⁵ Corroborating these studies, we found that a single i.c.v. administration of A β_{1-40} induces a rapid onset and sustained rise of MIP-1 α mRNA levels in the hippocampus. However, we failed to observe any significant alteration in the expression of CCR5 mRNA in response to A β_{1-40} , despite recent research showing increased CCR5 expression in A β -treated monocytes *in vitro*³⁹ and in reactive microglia of AD brains.¹¹

Several lines of evidence suggest a role for chemokines in AD. Besides CCR5, CCR2 and its ligand MCP-1 have also been identified as important regulators of microglia accumulation in AD. Overexpression of MCP-1 in mice expressing mutant amyloid precursor protein results in microglial accumulation in the brain. Nevertheless, these mice exhibit increased A β deposition.⁴⁰ Conversely, genetic deletion of CCR2 in mice expressing mutant amyloid precursor protein is associated with impaired microglial accumulation, accelerated A β deposition, and increased mortality.⁴¹ These discrepancies regarding the role played by chemokines in the progression of AD reinforce the need for additional studies describing the exact mechanisms regulating glial responses during the disease. In this sense, to determine whether the A β_{1-40} -induced MIP-1 α production resulted in accumulation of activated glial cells, we used immunohistochemical staining for GFAP, CD68, and Iba-1, well established markers for activated astrocytes and microglial cells.^{42,43} The results of the present study corroborate literature data, providing strong molecular evidence concerning the effect of A β intracerebral administration on glial cell activation in the CNS.^{20,38,44} We observed a striking increase in the number of activated astrocytes and microglial cells in response to A β_{1-40} . Moreover, our results demonstrate a critical role for MIP-1 α and CCR5 in this event, as genetic deletion or pharmacological blockage of the MIP-1 α /CCR5 pathway resulted in a marked reduction of GFAP- and CD68-, or Iba-1-positive cells in the hippocampuses of A β_{1-40} -treated mice. Using a model of neuroinflammation induced by LPS infusion, Rosi et al.²⁷ also found a marked reduction of activated microglia and astrocytes in the hippocampuses of rats treated with a CCR5 antagonist, confirming the important role played by this receptor in glial cell responses during CNS inflammation.

Inflammation in the AD brain has been reported in a number of studies.^{15,45} Interestingly, accumulating research has linked polymorphisms in cytokines and other immune molecules with AD, and epidemiological studies indicate that the use of nonsteroidal anti-inflammatory drugs reduces the risk of AD, thus reinforcing the notion that neuroinflammation can contribute to disease progression.^{46–49} In agreement with this hypothesis, we previously reported a correlation between TNF- α -related signaling pathways and iNOS expression, a crucial event for the decline in learning and memory functions induced by A β_{1-40} in mice.²⁰ The enzyme iNOS is not commonly

expressed in the CNS but can be induced after brain insult in astrocytes, microglia, neurons, and endothelial cells, where it catalyzes the production of high amounts of nitric oxide.^{50,51} Nitric oxide overproduction can in turn exacerbate neurodegeneration through the formation of peroxynitrite and protein nitration, affecting the physical and chemical nature of proteins.⁵² Moreover, transgenic mice expressing mutant human APP and presenilin-1 with genetic deletion of the iNOS gene are protected from premature mortality and cerebral plaque formation compared with their iNOS-expressing counterparts.⁵³ Herein, we demonstrated the involvement of MIP-1 α and CCR5 in A β_{1-40} -induced iNOS up-regulation, as we found reduced levels of the enzyme in MIP-1 $\alpha^{-/-}$ and CCR5 $^{-/-}$ mouse hippocampus. In addition to iNOS, one of the main proteins induced during inflammation is COX-2. COX enzymes are responsible for prostaglandin biosynthesis and are the primary target for nonsteroidal anti-inflammatory drugs.⁵⁴ Interestingly, studies conducted in AD brains have revealed increased COX-2 mRNA levels in the cortex⁵⁵ and hippocampus⁵⁶ and increased COX-2 protein expression in neurons and glial cells.^{55,57} Recently, studies conducted with genetically modified mice expressing mutant amyloid precursor protein and presenilin-1 have shown that the deletion of the prostaglandin E₂ EP₂ receptor reduces oxidative damage and amyloid burden.⁵⁸ COX-2 expression can also be induced in cultured microglia or astrocytes in response to A β .⁵⁹ Corroborating these results, our data demonstrate an inhibition of COX-2 up-regulation in the hippocampuses of MIP-1 $\alpha^{-/-}$ and CCR5 $^{-/-}$ mice, suggesting a role for these molecules in the modulation of COX-2 expression by A β_{1-40} . It is now well established that the increased expression of COX-2 and iNOS observed during inflammation is orchestrated by different transcription factors.^{60,61} In fact, we have previously demonstrated a critical role for CREB, NF- κ B, and AP-1 in the regulation of COX-2 and iNOS expression induced by A β_{1-40} in mouse hippocampus.²⁰ Herein, we found that the decrease in the expression of both enzymes in the hippocampuses of mice lacking MIP-1 α or CCR5 is associated with reduced activation of AP-1, NF- κ B, and CREB. Nevertheless, additional studies are necessary to establish the identity of the cells expressing activated transcription factors and COX-2 and/or iNOS proteins after A β_{1-40} treatment.

The absence of MIP-1 α and CCR5 could lead to decreased accumulation of activated glial cells accompanied by reduced inflammation through several possible mechanisms, including effects of MIP-1 α /CCR5 signaling on glial cell migration and/or activation. We therefore investigated each of these possibilities using *in vitro* assays. Notably, macrophages isolated from CCR5 $^{-/-}$ mice exhibited decreased migration in response to the supernatant of cells stimulated with A β_{1-40} . Furthermore, when MIP-1 $\alpha^{-/-}$ macrophages were stimulated with A β_{1-40} , their supernatant exerted reduced chemotactic activity, indicating that the production of MIP-1 α and the consequent activation of CCR5 are important events for cell migration induced by A β_{1-40} in mice. Of high interest, we found that A β_{1-40} and other stimuli such as LPS and C5a

were capable of inducing the production of IL-1 β and TNF- α in wild-type, MIP-1 $\alpha^{-/-}$, and CCR5 $^{-/-}$ cells in a comparable manner. Taken together, these results support a role for glial cells in neuroinflammation observed in this model of AD-like disease. However, despite the requirement of MIP-1 α and CCR5 for cell migration, these proteins seem not to be directly involved in the expression of inflammatory mediators induced by A β_{1-40} .

To evaluate whether the reduced glial cell accumulation and neuroinflammation observed in the absence of MIP-1 α and CCR5 were associated with decreased cognitive deficits in our model, we subjected animals to the spatial version of the water maze. As reported previously,²⁰⁻²² we observed a prominent impairment of learning and memory functions after a single i.c.v. injection of A β_{1-40} . Of great interest, our data show that MIP-1 $\alpha^{-/-}$ and CCR5 $^{-/-}$ mice are substantially protected against A β_{1-40} -induced learning and memory impairment. In addition, these effects seem to be related to an inhibition of the synaptic degeneration promoted by A β_{1-40} , because we found in MIP-1 $\alpha^{-/-}$ and CCR5 $^{-/-}$ mice synaptophysin levels comparable with those observed in PBS-treated mice. To our knowledge, this is the first *in vivo* evidence demonstrating a correlation between MIP-1 α /CCR5 signaling and the establishment of A β cognitive effects. In addition, probably by inhibiting the entry of HIV into microglia,⁶² the pharmacological blockade of CCR5 was associated with cognitive improvement in patients with AIDS, a disease that is also characterized by glial activation and extensive brain inflammation.⁶³

The relationship between chemokines and their receptors is complex, because individual chemokines can often bind to several different receptors, and a single chemokine receptor can be activated by multiple chemokines. Whereas CCR5 is responsible for some of the effects of MIP-1 α , MIP-1 β , and RANTES, MIP-1 α can also exert its actions through CCR1.³⁰ This promiscuity may account for the phenotypic differences between MIP-1 $\alpha^{-/-}$ and CCR5 $^{-/-}$ mice observed in our study, because MIP-1 β or RANTES could be activating CCR5 as well. However, additional studies are necessary to address the possible role played by these chemokines in A β_{1-40} -induced molecular and behavioral responses. Despite that the current results, together with data in the literature, provide clear functional and molecular evidence indicating that the chemokine system has a critical role in modulating the effects of A β , a process that could be of great relevance to the pathophysiology of AD.

References

1. Walsh DM, Selkoe DJ: Deciphering the molecular basis of memory failure in Alzheimer's disease. *Neuron* 2004, 44:181-193
2. González-Scarano F, Baltuch G: Microglia as mediators of inflammatory and degenerative diseases. *Annu Rev Neurosci* 1999, 22:219-240
3. Luster AD: Chemokines—chemotactic cytokines that mediate inflammation. *N Engl J Med* 1998, 338:436-445
4. Charo IF, Ransohoff RM: The many roles of chemokines and chemokine receptors in inflammation. *N Engl J Med* 2006, 354:610-621
5. Cartier L, Hartley O, Dubois-Dauphin M, Krause KH: Chemokine receptors in the central nervous system: role in brain inflammation and neurodegenerative diseases. *Brain Res Brain Res Rev* 2005, 48:16-42
6. Baggiolini M: Chemokines and leukocyte traffic. *Nature* 1998, 392:565-568
7. Ransohoff RM, Tani M, Glabinski AR, Chernosky A, Krivacic K, Peterson JW, Chien HF, Trapp BD: Chemokines and chemokine receptors in model neurological pathologies: molecular and immunocytochemical approaches. *Methods Enzymol* 1997, 287:319-348
8. Jiang Y, Salafranca MN, Adhikari S, Xia Y, Feng L, Sonntag MK, deFiebre CM, Pennell NA, Streit WJ, Harrison JK: Chemokine receptor expression in cultured glia and rat experimental allergic encephalomyelitis. *J Neuroimmunol* 1998, 86:1-12
9. Simpson JE, Newcombe J, Cuzner ML, Woodroffe MN: Expression of monocyte chemoattractant protein-1 and other β -chemokines by resident glia and inflammatory cells in multiple sclerosis lesions. *J Neuroimmunol* 1998, 84:238-249
10. Westmoreland SV, Rottman JB, Williams KC, Lackner AA, Sasseville VG: Chemokine receptor expression on resident and inflammatory cells in the brain of macaques with simian immunodeficiency virus encephalitis. *Am J Pathol* 1998, 152:659-665
11. Xia MQ, Qin SX, Wu LJ, Mackay CR, Hyman BT: Immunohistochemical study of the β -chemokine receptors CCR3 and CCR5 and their ligands in normal and Alzheimer's disease brains. *Am J Pathol* 1998, 153:31-37
12. McManus C, Berman JW, Brett FM, Staunton H, Farrell M, Brosnan CF: MCP-1, MCP-2 and MCP-3 expression in multiple sclerosis lesions: an immunohistochemical and in situ hybridization study. *J Neuroimmunol* 1998, 86:20-29
13. Klein RS, Williams KC, Alvarez-Hernandez X, Westmoreland S, Force T, Lackner AA, Luster AD: Chemokine receptor expression and signaling in macaque and human fetal neurons and astrocytes: implications for the neuropathogenesis of AIDS. *J Immunol* 1999, 163:1636-1646
14. Liu JX, Cao X, Tang YC, Liu Y, Tang FR: CCR7, CCR8, CCR9 and CCR10 in the mouse hippocampal CA1 area and the dentate gyrus during and after pilocarpine-induced status epilepticus. *J Neurochem* 2007, 100:1072-1088
15. Akiyama H, Barger S, Barnum S, Bradt B, Bauer J, Cole GM, Cooper NR, Eikelenboom P, Emmerling M, Fiebich BL, Finch CE, Frautschy S, Griffin WS, Hampel H, Hull M, Landreth G, Lue L, Mrak R, Mackenzie IR, McGeer PL, O'Banion MK, Pachter J, Pasinetti G, Plata-Salaman C, Rogers J, Rydel R, Shen Y, Streit W, Strohmeyer R, Tooyama I, Van Muiswinkel FL, Veerhuis R, Walker D, Webster S, Wegrzyniak B, Wenk G, Wyss-Coray T: Inflammation and Alzheimer's disease. *Neurobiol Aging* 2000, 21:383-421
16. Van Dam D, De Deyn PP: Drug discovery in dementia: the role of rodent models. *Nat Rev Drug Discov* 2006, 5:956-970
17. Sato N, Kuziel WA, Melby PC, Reddick RL, Kosteci V, Zhao W, Maeda N, Ahuja SK, Ahuja SS: Defects in the generation of IFN- γ are overcome to control infection with *Leishmania donovani* in CC chemokine receptor (CCR) 5-, macrophage inflammatory protein-1 α -, or CCR2-deficient mice. *J Immunol* 1999, 163:5519-5525
18. Cook DN, Beck MA, Coffman TM, Kirby SL, Sheridan JF, Pragnell IB, Smithies O: Requirement of MIP-1 α for an inflammatory response to viral infection. *Science* 1995, 269:1583-1585
19. El Khoury H, Hickman SE, Thomas CA, Cao L, Silverstein SC, Loike JD: Scavenger receptor-mediated adhesion of microglia to β -amyloid fibrils. *Nature* 1996, 382:716-719
20. Medeiros R, Prediger RD, Passos GF, Pandolfo P, Duarte FS, Franco JL, Dafre AL, Di Giunta G, Figueiredo CP, Takahashi RN, Campos MM, Calixto JB: Connecting TNF- α signaling pathways to iNOS expression in a mouse model of Alzheimer's disease: relevance for the behavioral and synaptic deficits induced by amyloid β protein. *J Neurosci* 2007, 27:5394-5404
21. Prediger RD, Franco JL, Pandolfo P, Medeiros R, Duarte FS, Di Giunta G, Figueiredo CP, Farina M, Calixto JB, Takahashi RN, Dafre AL: Differential susceptibility following β -amyloid peptide-(1-40) administration in C57BL/6 and Swiss albino mice: evidence for a dissociation between cognitive deficits and the glutathione system response. *Behav Brain Res* 2007, 177:205-213
22. Prediger RD, Medeiros R, Pandolfo P, Duarte FS, Passos GF, Pesquero JB, Campos MM, Calixto JB, Takahashi RN: Genetic deletion or antagonism of kinin B $_1$ and B $_2$ receptors improves cognitive deficits in a mouse model of Alzheimer's disease. *Neuroscience* 2008, 151:631-643

23. Town T, Laouar Y, Pittenger C, Mori T, Szekeley CA, Tan J, Duman RS, Flavell RA: Blocking TGF- β -Smad2/3 innate immune signaling mitigates Alzheimer-like pathology. *Nat Med* 2008, 14:681–687
24. Benes FM, Lange N: Two-dimensional versus three-dimensional cell counting: a practical perspective. *Trends Neurosci* 2001, 24:11–17
25. Mosmann T: Rapid colorimetric assay for cellular growth and survival: application to proliferation and cytotoxicity assays. *J Immunol Methods* 1983, 65:55–63
26. Morris RG, Garrud P, Rawlins JN, O'Keefe J: Place navigation impaired in rats with hippocampal lesions. *Nature* 1982, 297:681–683
27. Rosi S, Pert CB, Ruff MR, McGann-Gramling K, Wenk GL: Chemokine receptor 5 antagonist D-Ala-peptide T-amide reduces microglia and astrocyte activation within the hippocampus in a neuroinflammatory rat model of Alzheimer's disease. *Neuroscience* 2005, 134:671–676
28. Eberhardt W, Kunz D, Hummel R, Pfeilschifter J: Molecular cloning of the rat inducible nitric oxide synthase gene promoter. *Biochem Biophys Res Commun* 1996, 223:752–756
29. Kim Y, Fischer SM: Transcriptional regulation of cyclooxygenase-2 in mouse skin carcinoma cells. Regulatory role of CCAAT/enhancer-binding proteins in the differential expression of cyclooxygenase-2 in normal and neoplastic tissues. *J Biol Chem* 1998, 273:27686–27694
30. Viola A, Luster AD: Chemokines and their receptors: drug targets in immunity and inflammation. *Annu Rev Pharmacol Toxicol* 2008, 48:171–197
31. Rogers J, Lue LF: Microglial chemotaxis, activation, and phagocytosis of amyloid β -peptide as linked phenomena in Alzheimer's disease. *Neurochem Int* 2001, 39:333–340
32. Mennicken F, Maki R, de Souza EB, Quirion R: Chemokines and chemokine receptors in the CNS: a possible role in neuroinflammation and patterning. *Trends Pharmacol Sci* 1999, 20:73–78
33. Xia MQ, Hyman BT: Chemokines/chemokine receptors in the central nervous system and Alzheimer's disease. *J Neurovirol* 1999, 5:32–41
34. Fiala M, Zhang L, Gan X, Sherry B, Taub D, Graves MC, Hama S, Way D, Weinand M, Witte M, Lorton D, Kuo YM, Roher AE: Amyloid- β induces chemokine secretion and monocyte migration across a human blood-brain barrier model. *Mol Med* 1998, 4:480–489
35. Johnstone M, Gearing AJ, Miller KM: A central role for astrocytes in the inflammatory response to β -amyloid; chemokines, cytokines and reactive oxygen species are produced. *J Neuroimmunol* 1999, 93:182–193
36. Meda L, Baron P, Prat E, Scarpini E, Scarlato G, Cassatella MA, Rossi F: Proinflammatory profile of cytokine production by human monocytes and murine microglia stimulated with β -amyloid[25–35]. *J Neuroimmunol* 1999, 93:45–52
37. Lue LF, Rydel R, Brigham EF, Yang LB, Hampel H, Murphy GM Jr, Brachova L, Yan SD, Walker DG, Shen Y, Rogers J: Inflammatory repertoire of Alzheimer's disease and nondemented elderly microglia in vitro. *Glia* 2001, 35:72–79
38. El Khoury JB, Moore KJ, Means TK, Leung J, Terada K, Toft M, Freeman MW, Luster AD: CD36 mediates the innate host response to β -amyloid. *J Exp Med* 2003, 197:1657–1666
39. Giri RK, Rajagopal V, Shahi S, Zlokovic BV, Kalra VK: Mechanism of amyloid peptide induced CCR5 expression in monocytes and its inhibition by siRNA for Egr-1. *Am J Physiol Cell Physiol* 2005, 289:C264–C276
40. Yamamoto M, Horiba M, Buescher JL, Huang D, Gendelman HE, Ransohoff RM, Ikezu T: Overexpression of monocyte chemotactic protein-1/CCL2 in β -amyloid precursor protein transgenic mice show accelerated diffuse β -amyloid deposition. *Am J Pathol* 2005, 166:1475–1485
41. El Khoury J, Toft M, Hickman SE, Means TK, Terada K, Geula C, Luster AD: Ccr2 deficiency impairs microglial accumulation and accelerates progression of Alzheimer-like disease. *Nat Med* 2007, 13:432–438
42. Bignami A, Eng LF, Dahl D, Uyeda CT: Localization of the glial fibrillary acidic protein in astrocytes by immunofluorescence. *Brain Res* 1972, 43:429–435
43. Verbeek MM, Otte-Holler I, Wesseling P, Van Nostrand WE, Sorg C, Ruiters DJ, de Waal RM: A lysosomal marker for activated microglial cells involved in Alzheimer classic senile plaques. *Acta Neuropathol* 1995, 90:493–503
44. Yan JJ, Cho JY, Kim HS, Kim KL, Jung JS, Huh SO, Suh HW, Kim YH, Song DK: Protection against β -amyloid peptide toxicity in vivo with long-term administration of ferulic acid. *Br J Pharmacol* 2001, 133:89–96
45. Schwab C, McGeer PL: Inflammatory aspects of Alzheimer disease and other neurodegenerative disorders. *J Alzheimers Dis* 2008, 13:359–369
46. McDonald MP, Overmier JB, Bandyopadhyay S, Babcock D, Cleary J: Reversal of β -amyloid-induced retention deficit after exposure to training and state cues. *Neurobiol Learn Mem* 1996, 65:35–47
47. Rogers J, Kirby LC, Hempelman SR, Berry DL, McGeer PL, Kaszniak AW, Zalinski J, Cofield M, Mansukhani L, Willson P, Kogan F: Clinical trial of indomethacin in Alzheimer's disease. *Neurology* 1993, 43:1609–1611
48. Zandi PP, Breitner JC, Anthony JC: Is pharmacological prevention of Alzheimer's a realistic goal? *Expert Opin Pharmacother* 2002, 3:365–380
49. Wyss-Coray T: Inflammation in Alzheimer disease: driving force, bystander or beneficial response? *Nat Med* 2006, 12:1005–1015
50. Vallance P, Leiper J: Blocking NO synthesis: how, where and why? *Nat Rev Drug Discov* 2002, 1:939–950
51. Brown GC: Mechanisms of inflammatory neurodegeneration: iNOS and NADPH oxidase. *Biochem Soc Trans* 2007, 35:1119–1121
52. Koppal T, Drake J, Yatin S, Jordan B, Varadarajan S, Bettenhausen L, Butterfield DA: Peroxynitrite-induced alterations in synaptosomal membrane proteins: insight into oxidative stress in Alzheimer's disease. *J Neurochem* 1999, 72:310–317
53. Nathan C, Calingasan N, Nezezon J, Ding A, Lucia MS, La Perle K, Fuortes M, Lin M, Ehrt S, Kwon NS, Chen J, Vodovotz Y, Kipiani K, Beal MF: Protection from Alzheimer's-like disease in the mouse by genetic ablation of inducible nitric oxide synthase. *J Exp Med* 2005, 202:1163–1169
54. Mitchell JA, Akarasereenont P, Thiemermann C, Flower RJ, Vane JR: Selectivity of nonsteroidal antiinflammatory drugs as inhibitors of constitutive and inducible cyclooxygenase. *Proc Natl Acad Sci USA* 1993, 90:11693–11697
55. Pasinetti GM, Aisen PS: Cyclooxygenase-2 expression is increased in frontal cortex of Alzheimer's disease brain. *Neuroscience* 1998, 87:319–324
56. Ho L, Pieroni C, Winger D, Purohit DP, Aisen PS, Pasinetti GM: Regional distribution of cyclooxygenase-2 in the hippocampal formation in Alzheimer's disease. *J Neurosci Res* 1999, 57:295–303
57. Hoozemans JJ, Rozemuller AJ, Janssen I, De Groot CJ, Veerhuis R, Eikelenboom P: Cyclooxygenase expression in microglia and neurons in Alzheimer's disease and control brain. *Acta Neuropathol* 2001, 101:2–8
58. Liang X, Wang Q, Hand T, Wu L, Breyer RM, Montine TJ, Andreasson K: Deletion of the prostaglandin E₂ EP2 receptor reduces oxidative damage and amyloid burden in a model of Alzheimer's disease. *J Neurosci* 2005, 25:10180–10187
59. Hüll M, Muksch B, Akundi RS, Waschbisch A, Hoozemans JJ, Veerhuis R, Fiebich BL: Amyloid β peptide (25–35) activates protein kinase C leading to cyclooxygenase-2 induction and prostaglandin E₂ release in primary midbrain astrocytes. *Neurochem Int* 2006, 48:663–672
60. Tsatsanis C, Androulidaki A, Venihaki M, Margioris AN: Signalling networks regulating cyclooxygenase-2. *Int J Biochem Cell Biol* 2006, 38:1654–1661
61. Kleinert H, Pautz A, Linker K, Schwarz PM: Regulation of the expression of inducible nitric oxide synthase. *Eur J Pharmacol* 2004, 500:255–266
62. He J, Chen Y, Farzan M, Choe H, Ohagen A, Gartner S, Busciglio J, Yang X, Hofmann W, Newman W, Mackay CR, Sodroski J, Gabuzda D: CCR3 and CCR5 are co-receptors for HIV-1 infection of microglia. *Nature* 1997, 385:645–649
63. Heseltine PN, Goodkin K, Atkinson JH, Vitiello B, Rochon J, Heaton RK, Eaton EM, Wilkie FL, Sobel E, Brown SJ, Feaster D, Schneider L, Goldschmidts WL, Stover ES: Randomized double-blind placebo-controlled trial of peptide T for HIV-associated cognitive impairment. *Arch Neurol* 1998, 55:41–51